

Effect of multiple-pass friction stir processing on microstructure and tensile properties of a cast aluminum–silicon alloy

Z.Y. Ma^a, S.R. Sharma^b, R.S. Mishra^{b,*}

^a *Institute of Metal Research, Chinese Academy of Sciences, Shenyang 110016, China*

^b *Center for Friction Stir Processing and Department of Materials Science and Engineering, University of Missouri, 218 McNutt Hall, 1870 Miner Circles, Rolla, MO 65409, USA*

Received 2 December 2005; received in revised form 9 January 2006; accepted 11 January 2006

Available online 3 February 2006

Abstract

Five-pass friction stir processing (FSP), with 50% overlap, was conducted on cast A356. Overlapping FSP did not exert a significant effect on the size and distribution of the Si particles. In the as-FSP condition, the strength and ductility of the transitional zones between two FSP passes were slightly lower than those of the nugget zones. Further, in the multiple-pass material the strength of the previously processed zones was lower than that of the subsequent processed zones due to overaging from the FSP thermal cycles.

© 2006 Acta Materialia Inc. Published by Elsevier Ltd. All rights reserved.

Keywords: Friction stir processing; Cast A356; Overlapping passes; Multiple-pass; Aluminum alloy

1. Introduction

Friction stir processing (FSP) is a new solid-state processing technique for microstructural modification [1,2], which was developed based on the principle of friction stir welding (FSW) [3]. The basic concept of FSP is remarkably simple. A rotating tool with a pin and shoulder is inserted into a single piece of material and traversed along the desired path to cover the region of interest and this results in significant microstructural changes in the processed zone due to intense plastic deformation, mixing, and thermal exposure of material. The characteristics of FSP have led to several applications for microstructural modification in metallic materials, including enhanced superplasticity [1,2,4–7], surface composites [8], homogenization of nanophase aluminum alloys and metal matrix composites [9,10], and microstructural refinement of cast aluminum alloys [11–14].

Previous studies indicated that FSP resulted in a significant breakup of the coarse acicular Si particles and the pri-

mary aluminum dendrites, created a homogeneous distribution of Si particles in the aluminum matrix, and nearly eliminated all casting porosity in the sand-cast A356 [11–13]. These microstructural modifications significantly improved the mechanical properties of the cast A356, in particular the ductility and fatigue lifetime [11–13]. These observations indicated that FSP is an effective tool to modify the microstructure in the cast aluminum alloys.

Single-pass FSP with a pin diameter of 8 mm usually produces a processed zone with a width of 10–14 mm. Such a narrow processed zone might not be suitable for practical engineering applications. There are two approaches to increase the width of the processed zones. The first one is to use a large diameter pin. However, there is a limit to the pin size due to the capacity of the friction stir welding machine and the feasibility of producing a sound processed zone. The second one is to process the sample using multiple-pass FSP with a certain level of overlap between the successive passes. In this case, it is important to understand the microstructure evolution during the multiple-pass FSP and its influence on the mechanical properties.

* Corresponding author. Tel.: +1 573 341 6361; fax: +1 573 341 6934.
E-mail address: rsmishra@umr.edu (R.S. Mishra).

In a very recent study, Santella et al. [14] reported an improvement in the tensile strength of multiple-pass FSP A356 and A319 compared to the as-cast base metals. They used transverse tensile specimens with a gage length of 12.5 mm, which covered the whole FSP region produced by multiple-pass FSP. The larger tensile specimen geometry provides the overall response of overlap passes. While this is very useful for engineering applications, it does not provide an insight into the correlation between the intrinsic tensile properties and the localized microstructure. In this paper, we report the results of the effect of multiple-pass FSP on the microstructural modification of sand-cast A356 and the resultant tensile properties using mini-tensile specimens, in order to establish the relationship between the intrinsic tensile properties and the various microstructural regions.

2. Experimental

Sand-cast A356 plates of 15 mm thickness with a composition of 7.20Si–0.36Mg–0.13Fe–0.16Ti–bal Al (in wt.%) were used for this study. Five-pass FSP with a tool rotation rate of 700 rpm and a traverse speed of 203 mm/min was performed using a tri-flute pin. The overlap between the passes was one-half of the pin diameter. After each FSP pass, the plate was cooled down to room temperature and then the next FSP pass was performed to eliminate the effect of accumulative heating. The FSP sample was cut in the transverse direction, ground, polished, and examined using optical microscopy. The size and aspect ratio of the Si particles were analyzed by using Scion Image software. An equivalent diameter, D ($D = (d_L d_T)^{1/2}$), was used to define the size of the Si particles, where d_L and d_T are the dimensions of the major and minor axes of the particles, respectively. The aspect ratio of the Si particles is defined as the ratio of d_L and d_T .

The FSP sample was kept at room temperature for more than 1 month to naturally age after FSP. Part of the FSP sample was subjected to T6 tempering (solutionized at 540 °C/4 h, water quenched, and aged at 155 °C/4 h). To measure the mechanical properties of various microstructural zones, mini-tensile specimens with 1.3 mm gage length and 1.0 mm gage width were electro-discharge machined in the transverse direction from various locations. The specimens were ground and polished to a final thickness of ~0.5 mm, and then tested at an initial strain rate of $1 \times 10^{-3} \text{ s}^{-1}$ using a computer-controlled, custom-built mini-tensile tester. The average tensile property for each condition was obtained by averaging five test results.

3. Results and discussion

3.1. Microstructure

Fig. 1 shows a macrograph of 5-pass FSP A356. Various microstructural regions are distinctly visible. The remnant regions of the nugget zones from the first to the fourth pass

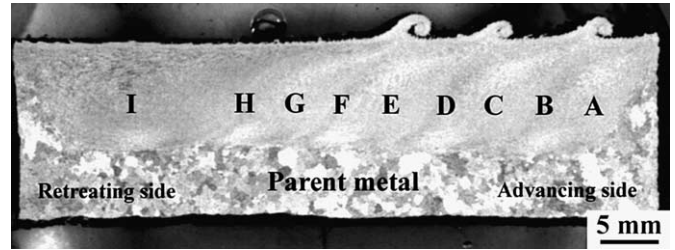


Fig. 1. Macrographs showing nugget and transitional zones of 5-pass FSP A356.

FSP are labeled as A, C, E, and G in Fig. 1 (hereafter referred to as the 1st, 2nd, 3rd, and 4th pass nugget zones). The transition regions between two FSP passes are labeled as B, D, F, and H in Fig. 1 (hereafter referred to as the 1st–2nd, 2nd–3rd, 3rd–4th, and 4th–5th pass transitional zones), and the nugget zone of the 5th pass FSP as I in Fig. 1 (hereafter referred to as the 5th pass nugget zone). In the transitional boundaries between two FSP passes, the metal flow lines are clearly visible.

Optical microscopic examinations show that the size and distribution of the Si particles in various microstructural regions, i.e., around locations A, B, C, D, E, F, G, H, and I in Fig. 1 are similar, and the Si particle distribution in various regions is quite uniform. Fig. 2 presents typical micrographs showing the Si particle distribution in locations A, D, and I. The size and aspect ratio of the Si particles in various regions are summarized in Table 1. For comparison, the data for the as-cast alloy and the single-pass FSP A356, prepared with the same FSP tool geometry and parameters, are also included in Table 1. The size and aspect ratio of the Si particles in various regions are quite similar, indicating that overlapping FSP did not result in further breakup of the Si particles. Furthermore, the size and aspect ratio of the Si particles in various regions for the 5th pass FSP sample are in good agreement with those achieved for the single-pass FSP sample.

3.2. Tensile properties

Fig. 3 shows the tensile properties of various microstructural regions in the 5-pass FSP A356 sample. For comparison, the tensile properties of the as-cast alloy and the single-pass FSP A356, prepared with same FSP tool geometry and parameters, are listed in Table 2. Under the as-FSP condition, the following observations can be made from Fig. 3 and Table 2. First, the strength and ductility of the transitional zones are lower than those of the nugget zones. Second, generally, the strengths of both nugget and transitional zones decrease with increasing distance from the 5th pass processed zone. Third, both the strength and ductility of the 5th pass FSP nugget zone are similar to those achieved in the single-pass FSP sample. Furthermore, both the tensile and yield strengths of various microstructural regions in the present 5-pass FSP A356 achieved by mini-tensile specimens are higher than those for large

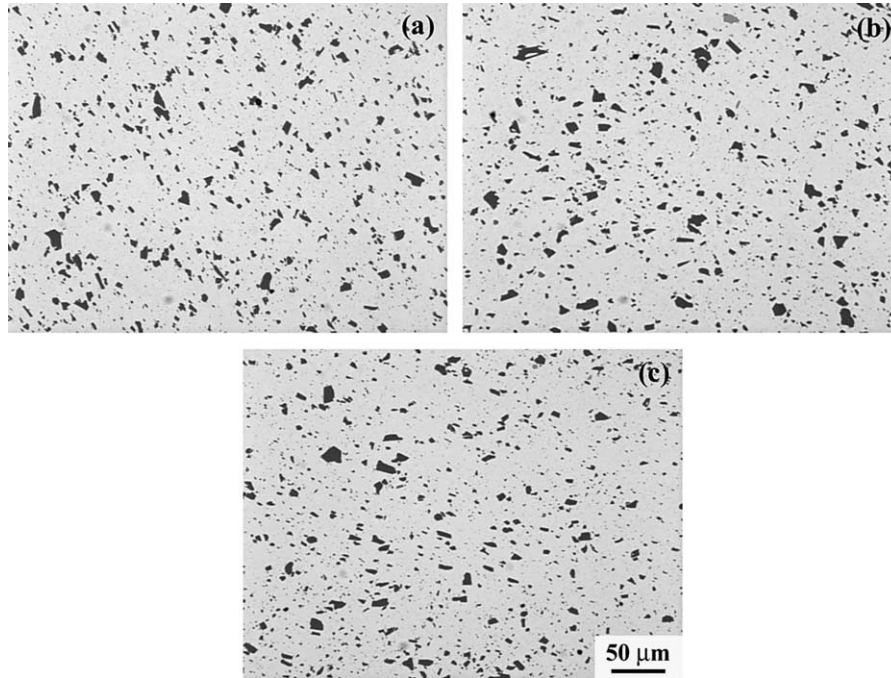


Fig. 2. Typical optical micrographs showing Si particle distribution in 5-pass FSP A356: (a) 1st pass, (b) 2nd–3rd pass transition, and (c) 5th pass (locations A, D, and I in Fig. 1).

Table 1
Size and aspect ratio of Si particles in 5-pass FSP A356

Processing condition	Location	Particle size (μm)	Aspect ratio
5th pass FSP	Point A, 1st pass	2.47 ± 1.89	1.96 ± 0.92
	Point B, 1st–2nd pass transition	2.56 ± 2.17	1.84 ± 0.74
	Point C, 2nd pass	2.52 ± 2.08	1.85 ± 0.76
	Point D, 2nd–3rd pass transition	2.43 ± 1.89	1.90 ± 0.86
	Point E, 3rd pass	2.54 ± 1.97	1.83 ± 0.77
	Point F, 3rd–4th pass transition	2.40 ± 1.88	1.90 ± 0.81
	Point G, 4th pass	2.38 ± 1.82	1.85 ± 0.77
	Point H, 4th–5th pass transition	2.24 ± 1.69	1.85 ± 0.75
	Point I, 5th pass	2.37 ± 1.89	1.85 ± 0.74
Cast		16.75 ± 9.21	5.92 ± 4.34
Single-pass FSP	Nugget center	2.48 ± 2.02	1.94 ± 0.88

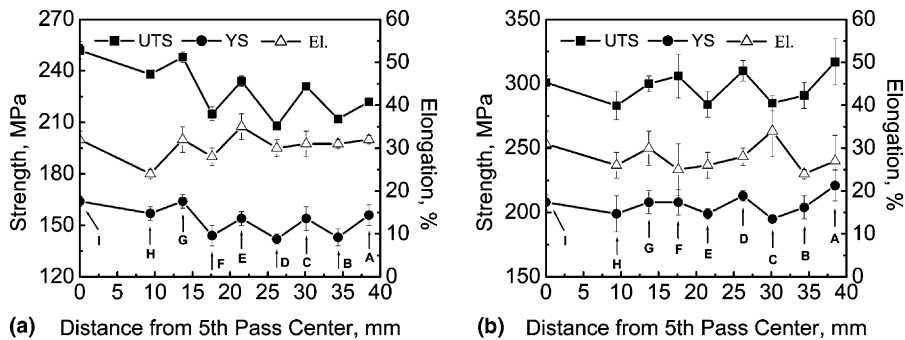


Fig. 3. Tensile properties of various microstructural zones in 5-pass FSP A356 sample as a function of distance from the 5th pass center: (a) as-FSP and (b) T6-treated (A, B, C, D, E, F, G, H, and I correspond to locations A, B, C, D, E, F, G, H, and I in Fig. 1).

specimens in Ref. [14]. This shows that the FSP parameters and tool design can influence the level of improvement of the mechanical properties.

Fig. 2 and Table 1 show that the size and aspect ratio, as well as the distribution of the Si particles, are quite similar in various microstructural regions of the 5-pass FSP A356

Table 2
Tensile properties of as-cast and single-pass FSP A356 at room temperature ($\dot{\epsilon} = 10^{-3} \text{ s}^{-1}$)

Processing condition	As-FSP or as-received			T6-treated		
	UTS (MPa)	YS (MPa)	El. (%)	UTS (MPa)	YS (MPa)	El. (%)
As-cast	169 ± 8	132 ± 3	3 ± 1	220 ± 10	207 ± 7	2 ± 1
Single-pass FSP	251 ± 4	171 ± 12	31 ± 1	301 ± 6	216 ± 11	28 ± 2

UTS: ultimate tensile strength; YS: yield strength; El.: elongation.

sample. Thus, the difference between the tensile properties of the transitional and nugget zones cannot be attributed to the Si particles. The reason for the slight reduction in strength in the transition zones is not clear. One possibility is that the strengthening precipitates, Mg_2Si , in the transition region go through additional coarsening.

FSW/FSP results in an intense temperature rise of 400–500 °C [15–17]. Thus, during the FSP thermal cycle most of the Mg_2Si precipitates, the primary strengthening phase in A356, dissolved into the aluminum matrix [13]. Fast cooling from the FSP thermal cycle retains these solutes in solution. In this case, precipitation occurred during the room temperature natural aging after FSP, resulting in an increase in the strength of the FSP samples [13]. However, when performing multiple-pass FSP, each subsequent FSP pass causes a short-term high temperature exposure of the previously processed zones, resulting in overaging of these zones. Post-FSP room temperature aging can strengthen the as-FSP sample due to precipitation, but does not exert any significant effect on the overaged microstructure. Therefore, the strength of the previously processed zones is lower than that of the subsequently processed zones. Among the five nugget zones, the 1st pass nugget zone exhibits the lowest strength as it underwent the maximum number of high-temperature thermal cycles.

Fig. 3 shows that T6-treatment results in a significant increase in both yield and ultimate tensile strengths and a slight decrease in ductility for various microstructural zones of the 5-pass FSP A356 sample. This is due to the complete dissolution of the Mg_2Si precipitates during the solid-solution treatment and the subsequent re-precipitation during the T6-aging. It is noted from Fig. 3 that both strength and ductility are scattered within a band for various microstructural zones and no systematic variation is observed. This indicates that the T6-heat treatment removes the thermal effects in the multiple-pass FSP A356 sample and produces a similar microstructure across various passes. Further, the 5-pass FSP sample in various microstructural regions exhibits strength and ductility values comparable to those achieved in the single-pass FSP sample (Table 2). This indicates that multiple-pass FSP with a 50% overlap is a feasible route to perform microstructural modification on large-sized aluminum castings.

4. Conclusions

1. Overlapping FSP did not affect the size, aspect ratio, and distribution of the Si particles. The Si particles broken by FSP were uniformly distributed in the entire processed zones created by multiple-pass FSP.
2. Under the as-FSP condition, both the strength and ductility of the transitional zones were lower than those of the nugget zones. The strength of the previous FSP zones was lower than that of the subsequent FSP zones.
3. After T6-heat treatment, the tensile properties of the 5-pass FSP A356 samples were similar across various passes and comparable to those of the single-pass FSP sample.

Acknowledgements

This work was supported by (a) the National Science Foundation through Grant DMR-0076433 and the Missouri Research Board in the acquisition of a friction stir welding and processing machine and (b) DARPA under Contract No. MDA972-02-C-0030. One of the authors (Z.Y.M.) gratefully acknowledges the support of the Hundred Talents Project of the Chinese Academy of Sciences and the National Outstanding Young Scientist Foundation under Grant No. 50525103.

References

- [1] Mishra RS, Mahoney MW, McFadden SX, Mara NA, Mukherjee AK. Scripta Mater 2000;42:163.
- [2] Mishra RS, Mahoney MW. Mater Sci Forum 2001;357-3:507.
- [3] Thomas WM, Nicholas ED, Needham JC, Murch MG, Templesmith P, Dawes CJ. GB Patent Application No. 9125978.8; Dec. 1991.
- [4] Ma ZY, Mishra RS, Mahoney MW. Acta Mater 2002;50:4419.
- [5] Ma ZY, Mishra RS, Mahoney MW. Scripta Mater 2004;50:931.
- [6] Ma ZY, Mishra RS. Scripta Mater 2005;53:75.
- [7] Ma ZY, Mishra RS, Mahoney MW, Grimes R. Metall Mater Trans 2005;A36:1147.
- [8] Mishra RS, Ma ZY, Charit I. Mater Sci Eng 2003;A34:307.
- [9] Berbon PB, Bingel WH, Mishra RS, Bampton CC, Mahoney MW. Scripta Mater 2001;44:61.
- [10] Spowart JE, Ma ZY, Mishra RS. In: Jata KV, Mahoney MW, Mishra RS, Semiatin SL, Lienert T, editors. Friction stir welding and processing II. Warrendale, PA: TMS; 2003. p. 243–52.
- [11] Ma ZY, Sharma SR, Mishra RS, Mahoney MW. Mater Sci Forum 2003;426–432:2891.
- [12] Sharma SR, Ma ZY, Mishra RS. Scripta Mater 2004;51:237.
- [13] Ma ZY, Sharma SR, Mishra RS. Metall Mater Trans, submitted for publication.
- [14] Santella ML, Engstrom T, Storzjohann D, Pan TY. Scripta Mater 2005;53:201.
- [15] Mahoney MW, Rhodes CG, Flintoff JG, Spurling RA, Bingel WH. Metall Mater Trans 1998;A29:1955.
- [16] Mishra RS, Ma ZY. Mater Sci Eng R 2005;50:1.
- [17] Tang W, Guo X, McClure JC, Murr LE. J Mater Process Manuf Sci 1998;7:163.